ChemComm

COMMUNICATION

View Article Online
View Journal | View Issue

Cite this: *Chem. Commun.*, 2014, 50, 4856

Received 6th February 2014,
Accepted 19th March 2014

DOI: 10.1039/c4cc00971a

www.rsc.org/chemcomm

Elucidating proline dynamics in spider dragline silk fibre using ^{2}H–^{13}C HETCOR MAS NMR†

Xiangyan Shi, Jeffery L. Yarger* and Gregory P. Holland*

^{2}H–^{13}C HETCOR MAS NMR is performed on $^{2}H/^{13}C/^{15}N$-Pro enriched *A. aurantia* dragline silk. Proline dynamics are extracted from ^{2}H NMR line shapes and T_1 in a site-specific manner to elucidate the backbone and side chain molecular dynamics for the MaSp2 GPGXX β-turn regions for spider dragline silk in the dry and wet, supercontracted states.

Orb-weaving dragline silk fibre possesses outstanding mechanical properties – a combination of stiffness, toughness and extensibility.[1,2] Two proteins, major ampullate spidroin 1 and major ampullate spidroin 2 (MaSp1 and MaSp2), are the primary components of dragline silk from most orb-weaving spiders, including *A. aurantia* (a common garden spider collected in California).[3] MaSp1 and 2 are composed of highly repetitive amino acid motifs with unique secondary structures.[2,4–8] Solid-state NMR revealed that poly-Ala (typically 5–8 Ala units long) and poly-(Gly-Ala) motifs found in both MaSp1 and 2 proteins are arranged into β-sheet structures in spider silk fibres, and are believed to be the primary source of fibre strength and stiffness.[4,5,8] Gly-Gly-X domains form disordered 3_1-helical structures and are primarily found in MaSp1.[4,5,8] While Gly-Pro-Gly-XX (GPGXX) domains are exclusively found in MaSp2 and form disordered type II β-turn structures, thought to be partially responsible for dragline spider silk's extensibility.[6] When exposed to water, spider dragline silk shrinks up to 50% in length and swells in diameter.[9,10] This phenomenon is known as supercontraction and is accompanied by a decrease in fibre stiffness and loss of molecular structural order along the fibre axis.[9–12] Previous studies suggest that silk supercontraction correlates to its Pro content.[13] Pro residues reside exclusively in the GPGXX motif.[3] Understanding the dynamics of proline, and hence the GPGXX domain in MaSp2, will provide insight into the supercontraction mechanism and the silk's extensibility.

Deuterium (^{2}H) NMR line shapes and spin–lattice relaxation times (T_1) provide extensive information about molecular dynamics and geometry.[14] One-dimensional (1D) ^{2}H experiments exhibit poor resolution caused by the large quadrupolar interaction and small chemical shift dispersion. Furthermore, labelling ^{2}H at specific groups is difficult or impossible for natural biopolymers.[15] Our research group has recently developed a two-dimensional (2D) ^{2}H–^{13}C heteronuclear correlation (HETCOR) magic angle spinning (MAS) NMR technique for extracting site-specific ^{2}H line shapes for systems with multiple isotope labelled sites.[16] The HETCOR NMR experiment was accomplished using cross-polarization (CP)-MAS under carefully calibrated experimental conditions. Further, a method was developed to indirectly measure ^{2}H T_1 through ^{2}H–^{13}C CP-MAS in a site-specific manner and was successfully applied to several model systems.[16] *A. aurantia* dragline silk was chosen for this study, because it contains a high abundance of MaSp2, and therefore it is more Pro-rich compared to the other dragline silks.[17] In present work, ^{2}H–^{13}C HETCOR MAS experiments were performed on dragline silk collected from spiders fed with a U-[$^{2}H_7$,$^{13}C_5$,^{15}N]-Pro aqueous solution. Pro molecular dynamics were probed for both dry (native material) and supercontracted (wet) dragline spider silks.

1D liquid-state ^{2}H NMR shows that Pro side-chain CD_2 groups and backbone CD were labelled by ^{2}H for the silk samples (Fig. S1, ESI†). The ^{2}H *J*-splitting patterns indicate that all the ^{2}H labelled groups were also enriched with ^{13}C. This selective amino acid labelling with ^{2}H–^{13}C pairs is ideal for 2D HETCOR MAS NMR experiments for dynamic studies. HETCOR MAS NMR experiments were performed on this dragline silk. A 2D NMR experiment with a small spectral window and rotor-synchronized sampling in the ^{2}H dimension was performed to obtain a ^{2}H–^{13}C chemical shift correlation spectrum (Fig. 1). As shown in the projection of the spectrum, ^{13}C signals were assigned to each Pro group based on the chemical shifts reported in previous studies.[6] The ^{2}H–^{13}C correlation was only observed

Department of Chemistry and Biochemistry, Magnetic Resonance Research Center, Arizona State University, Tempe, AZ 85287-1604, USA.
E-mail: greg.holland@asu.edu, jyarger@gmail.com

† Electronic supplementary information (ESI) available: Materials and methods, liquid-state ^{2}H spectrum of hydrolyzed *A. aurantia* dragline silk, simulated ^{2}H quadrupole line shapes, ^{13}C-detected Pro ^{2}H T_1 inversion recovery curves, calculating molecular motional rate using ^{2}H T_1, ^{2}H one-pulse spectrum and its fit. See DOI: 10.1039/c4cc00971a

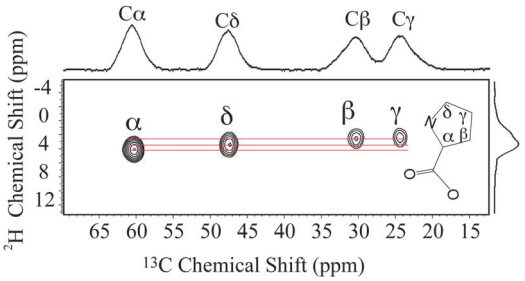

Fig. 1 ^{2}H–^{13}C HETCOR MAS spectrum for U-[^{2}H$_7$,^{13}C$_5$,^{15}N]-Pro labelled *A. aurantia* dragline silk. Rotor-synchronized sampling in the indirect dimension was used to eliminate spinning sidebands and obtain a narrow spectral-width high-resolution spectrum. The ^{2}H–^{13}C correlation is indicated for each Pro site in the spectrum (red lines).

between directly bonded spin pairs, illustrating the site-specific nature of the HETCOR MAS NMR experiment.

^{2}H line shapes were extracted from a 2D NMR experiment with a ^{2}H spectral window larger than the deuterium quadrupolar interaction. The spectrum and extracted ^{2}H line shapes are displayed in Fig. 2. Pro side-chain molecular motion can be described by each CD_2 undergoing a two-site reorientation. To interpret this motion for each site, ^{2}H line shape simulations were conducted and compared with the experimental data (see ESI†). It reveals that each deuterium on the side-chain undergoes fast two-site reorientation at an angle of 10–15°, 15–20° and 5–10° for Pro ^{2}Hβ, ^{2}Hγ and ^{2}Hδ, respectively (Fig. 2(b)). The corresponding reorientation rates are greater than 10^8 s^{-1}. Pro residues in spider dragline silk (GPGXX motif) have much smaller reorientation

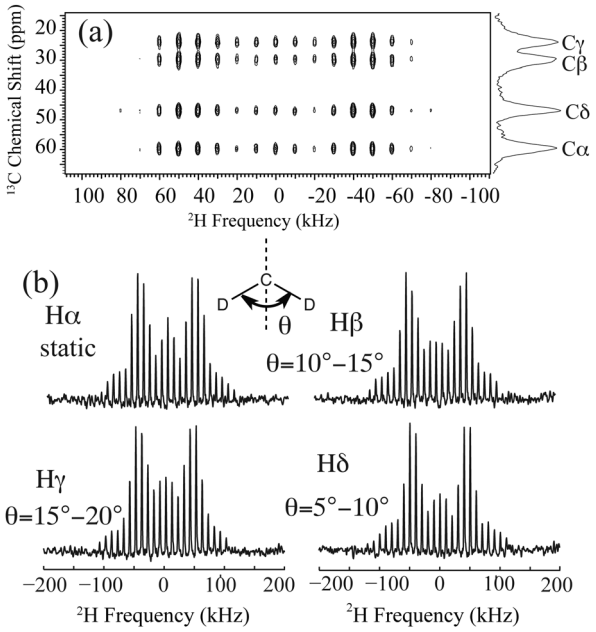

Fig. 2 (a) ^{2}H–^{13}C HETCOR MAS NMR spectrum for U-[^{2}H$_7$,^{13}C$_5$,^{15}N]-Pro labelled *A. aurantia* dragline silk. (b) Pro ^{2}H line shapes extracted from the 2D spectrum and the proposed dynamics for each site. Pro side-chain dynamics is described by each CD_2 undergoing fast reorientation between two sites separated by an angle θ. The angles are extracted from comparing experimental ^{2}H line shapes with simulations (see ESI†).

angles when compared to crystalline proline.[16,19] A static MAS pattern was observed for Pro ^{2}Hα, illustrating the rigidity of the Pro backbone environment ($<10^2$ s^{-1}) in dry spider dragline silk.

The molecular dynamics of the Pro side-chain was determined to be $>10^8$ s^{-1}, however, ^{2}H line shape cannot provide the exact motional rate. ^{2}H T_1 is another NMR tool for characterizing the molecular motion on the picosecond – nanosecond timescale. In the current work, site-specific ^{2}H T_1 was indirectly measured through ^{13}C-detected ^{2}H–^{13}C CP-MAS experiments. ^{2}H T_1's were determined to be 613 ms, 569 ms, 573 ms and 561 ms for Pro ^{2}Hα, ^{2}Hβ, ^{2}Hγ and ^{2}Hδ, respectively (Fig. S3, ESI†). The quadrupolar interaction is the dominant ^{2}H T_1 relaxation mechanism and has been hypothesized as the only relevant relaxation source when investigating ^{2}H dynamics for various systems.[7,20,21] If only the ^{2}H quadrupolar interaction is considered, a two-site reorientation rate of 1.4×10^{10} s^{-1}, 2.6×10^{10} s^{-1} and 5.3×10^9 s^{-1} is determined from the corresponding deuterium T_1 for Pro ^{2}Hβ, ^{2}Hγ and ^{2}Hδ, respectively (see ESI† for calculation detail). When the silk is wet and supercontracted, ^{2}H–^{13}C CP signal was undetectable with reasonable NMR experimental time because of inefficient CP. This indicates that the Pro-containing motifs interact strongly with water molecules when the silk is supercontracted and exhibit mobility that completely averages the ^{2}H–^{13}C dipolar interaction that facilitates CP.

1D ^{2}H solid-echo (Fig. 3) and one-pulse (Fig. S4, ESI†) MAS NMR experiments were conducted to probe Pro dynamics in the wet, supercontracted silk. These experiments illustrate that the large Pro ^{2}H spinning sideband (SSBs) pattern observed in dry silk are reduced to a central peak accompanied by one set of weak SSBs when the silk is wet. Significant signal loss was observed for the supercontracted silk in fully relaxed ^{2}H solid-echo and one-pulse MAS NMR spectra (Fig. 3a and Fig. S4, ESI†) compared to the dry silk. For the wet supercontracted silk, the central peak cannot be fit by one peak possessing a Lorentzian, Gaussian or combined lineshape. Instead, fits of ^{2}H 1D data indicate the existence of two components, a broad (~3.8 kHz FWHM) and narrow peak (~400 Hz FWHM) (Fig. 3b and Fig. S4, ESI†). The broad component is indicative of microsecond dynamics for a Pro deuterium population. This dynamical process could be the motion of the Pro local backbone as no additional bond on the side-chain is available for the CD_2 undergoing another motion besides the fast two-site reorientations. This backbone motion can be described by a simple model where the entire Pro residue undergoes three site reorientation along an external axis with a rate of 3×10^6 s^{-1} (Fig. 3c). The axis is considered the long axis of the local protein backbone. The observed ^{2}H signal loss is due to the short T_2 of the broad component, a consequence of molecular dynamics in the microsecond regime. In contrast, the narrow component obtained from the fit corresponds to a Pro population that becomes extremely mobile due to strong interactions with water. This Pro mobile population accounts for 30–35% based on the signal loss of ^{2}H 1D data of supercontracted silk compared to dry silk and the peak deconvolution (Fig. 3b and Fig. S4, ESI†). Thus, 65–70% of the Pro residues undergo 3×10^6 s^{-1} backbone motions when silk is wet and supercontracted. As the protein

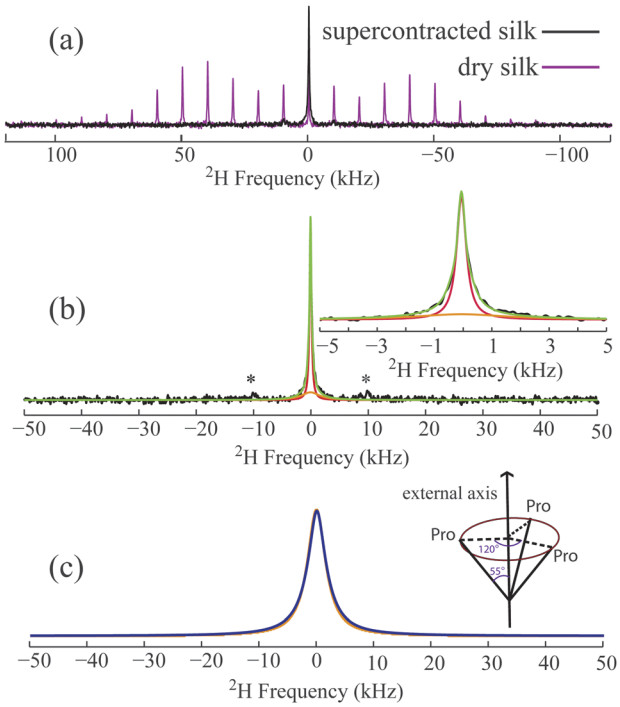

Fig. 3 (a) ^{2}H solid-echo MAS NMR spectra for U-[$^{2}H_{7}$,$^{13}C_{5}$,^{15}N]-Pro labelled *A. aurantia* dragline silk in the dry and supercontracted (wet) state. (b) ^{2}H solid-echo MAS spectrum of supercontracted (wet) silk (black, same one as show in (a) and its fit (green)). The central peak region is expanded and shown on the upper right. A broad (orange) and narrow (red) component was used for the fit. The asterisks indicate the spinning sidebands. (c) Experimental (orange) and simulated ^{2}H line shape (blue). The experimental line shape is the broad component extracted from the fit (shown in orange in b). Simulations were performed using SPINEVOLUTION[18] with a model of the entire Pro residue undergoing a three-site reorientation along an external axis with a rate of 3×10^{6} s^{-1} (the schematic representation of the motion is show on the upper right).

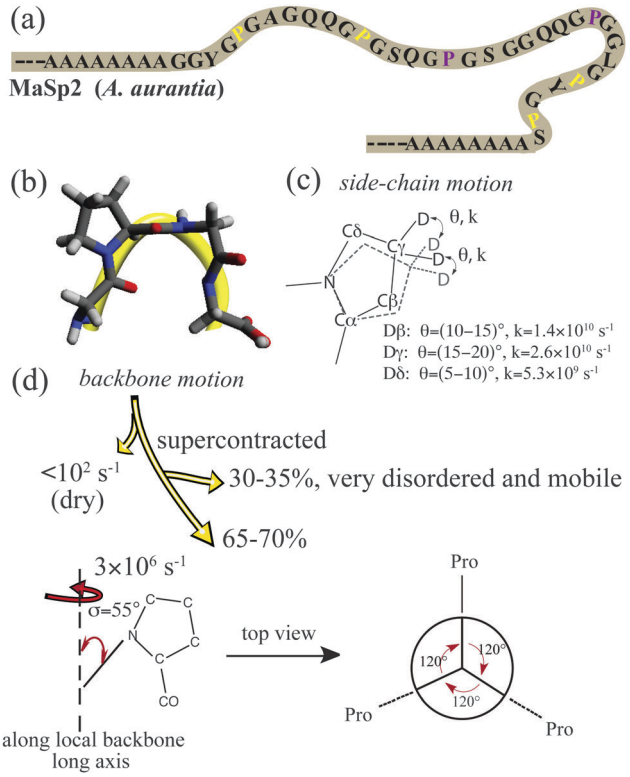

Fig. 4 Proposed protein backbone and side-chain dynamics for Pro-containing motifs in *A. aurantia* dragline silk fibre. (a) Primary amino acid sequence of MaSp2 repetitive motifs. (b) Schematic representation of type II β-turn structure for Pro-rich motif. The shown structural element is Gly-Pro-Gly-Ala. (c) Pro side-chain dynamics in the native, dry silk fibre where the Pro side-chain CD_2 undergo fast reorientation between two sites separated by an angle θ. Pro side-chains become much more mobile when the silk is wet, supercontracted (not shown). (d) Backbone dynamics. For wet, supercontracted silk, 65–70% of Pro-containing regions (highlighted in yellow in a) exhibit 3×10^{6} s^{-1} backbone motion. The mobility of the remaining 30–35% Pro-rich regions (highlighted in purple in a) is near isotropic.

exhibits much higher mobility for supercontracted (wet) silk, the exact dynamical time scale for the Pro side-chain could not be extracted from T_1, that is no longer dominated by the ^{2}H quadrupolar interaction.

Pro residues exist exclusively in the MaSp2 protein and within the GPGXX motif. From the primary protein sequence, the GPGXX motifs typically repeat 3–5 times and are sandwiched between the poly-Ala and poly-(Gly-Ala) domains that form rigid β-sheets.[3,8] Hence, it is reasonable to propose that the GPGXX motifs close to β-sheet regions (within two repeats) exhibit microsecond motions when the silk is supercontracted, because the dynamics are likely restricted by the flanking rigid β-sheet crystalline domains. In contrast, hydrated GPGXX motifs located further away from the β-sheet regions (>2 repeat units) are less constrained by the crystalline regions and undergo much faster, near isotropic motion. Combining the silk protein primary sequence with the molecular motion revealed by ^{2}H NMR, a model is proposed for Pro side-chain and the local protein backbone dynamics in dry and wet, supercontracted silk (Fig. 4).

In the current work, molecular dynamics for the GPGXX regions in spider dragline silk were investigated with ^{2}H–^{13}C HETCOR MAS NMR. In native (dry) dragline silk, the local backbone dynamics appears static (<10^{2} s^{-1}), while the side-chains undergo fast two-site reorientations in the >10^{9} s^{-1} regime. For supercontracted (wet) silk, two different molecular motions are observed for the GPGXX units in MaSp2 from ^{2}H MAS NMR: 65–70% of the GPGXX regions exhibit 3×10^{6} s^{-1} backbone motion, while the rest behave near isotropic. These two Pro populations are proposed to be within two units of the β-sheet domains and greater than two units from these rigid regions, respectively.

This work was supported by grants from AFOSR (FA9550-14-1-0014), DURIP (FA2386-12-1-3031 DURIP 12RSL231) and NSF (DMR-1264801). We would also like to thank Dr Brian Cherry for help with NMR instrumentation and student training.

Notes and references

1 J. M. Gosline, M. W. Denny and M. E. Demont, *Nature*, 1984, **309**, 551–552.
2 R. V. Lewis, *Chem. Rev.*, 2006, **106**, 3762–3774.
3 J. Gatesy, C. Hayashi, D. Motriuk, J. Woods and R. Lewis, *Science*, 2001, **291**, 2603–2605.
4 J. D. van Beek, S. Hess, F. Vollrath and B. H. Meier, *Proc. Natl. Acad. Sci. U. S. A.*, 2002, **99**, 10266–10271.

5 G. P. Holland, J. E. Jenkins, M. S. Creager, R. V. Lewis and J. L. Yarger, *Chem. Commun.*, 2008, 5568–5570.
6 J. E. Jenkins, M. S. Creager, E. B. Butler, R. V. Lewis, J. L. Yarger and G. P. Holland, *Chem. Commun.*, 2010, **46**, 6714–6716.
7 A. H. Simmons, C. A. Michal and L. W. Jelinski, *Science*, 1996, **271**, 84–87.
8 G. P. Holland, M. S. Creager, J. E. Jenkins, R. V. Lewis and J. L. Yarger, *J. Am. Chem. Soc.*, 2008, **130**, 9871–9877.
9 R. W. Work, *J. Exp. Biol.*, 1985, **118**, 379–404.
10 Y. Liu, Z. Shao and F. Vollrath, *Nat. Mater.*, 2005, **4**, 901–905.
11 Z. Shao, F. Vollrath, J. Sirichaisit and R. J. Young, *Polymer*, 1999, **40**, 2493–2500.
12 Z. T. Yang, O. Liivak, A. Seidel, G. LaVerde, D. B. Zax and L. W. Jelinski, *J. Am. Chem. Soc.*, 2000, **122**, 9019–9025.
13 Y. Liu, A. Sponner, D. Porter and F. Vollrath, *Biomacromolecules*, 2008, **9**, 116–121.
14 D. A. Torchia, *Annu. Rev. Biophys. Bioeng.*, 1984, **13**, 125–144.
15 X. Shi, J. L. Yarger and G. P. Holland, *Anal. Bioanal. Chem.*, 2013, **405**, 3997–4008.
16 X. Shi, J. L. Yarger and G. P. Holland, *J. Magn. Reson.*, 2013, **226**, 1–12.
17 A. E. Brooks, H. B. Steinkraus, S. R. Nelson and R. V. Lewis, *Biomacromolecules*, 2005, **6**, 3095–3099.
18 M. Veshtort and R. G. Griffin, *J. Magn. Reson.*, 2006, **178**, 248–282.
19 S. K. Sarkar, P. E. Young and D. A. Torchia, *J. Am. Chem. Soc.*, 1986, **108**, 6459–6464.
20 D. A. Torchia and A. Szabo, *J. Magn. Reson.*, 1982, **49**, 107–121.
21 L. S. Batchelder, C. H. Niu and D. A. Torchia, *J. Am. Chem. Soc.*, 1983, **105**, 2228–2231.